

SETI: The transmission rate of radio communication and the signal's detection

P. A. Fridman

ASTRON, Oude Hoogevensedijk 4, 7991PD Dwingeloo, The Netherlands

Abstract

The transmission rate of communication between radio telescopes on Earth and extraterrestrial intelligence (ETI) is here calculated up to distances of 1000 light years. Both phase-shift-keying (PSK) and frequency-shift keying (FSK) modulation schemes are considered. It is shown that M-ary FSK is advantageous in terms of energy. Narrow-band pulses scattered over the spectrum sharing a common drift rate can be the probable signals of ETI. Modern SETI spectrum analyzers are well suited to searching for these types of signals. Such signals can be detected using the Hough transform which is a dedicated tool for detecting patterns in an image. The time-frequency plane representing the power output of the spectrum analyzer during the search for ETI gives an image from which the Hough transform (HT) can detect signal patterns with frequency drift.

Keywords: SETI; communication; transmission rate; Hough transform

1. Introduction

Up until the present day searches have been undertaken for signals of two types of extra-terrestrial intelligence (ETI): monochromatic (continuous wave, CW) and pulses, [1], [2]. The detection of any such signal is presumed to be a demonstration of the existence of ETI. The signals are expected from both planetary systems similar to our Solar system and from beacons scattered across our Galaxy.

During the search for extraterrestrial intelligence (SETI), both targeted searches and sky surveys have been performed to detect narrow-band or pulse-like signals, [2]. The signals are examined by multi-channels spectrum analyzers. There can be millions of such channels and the bandwidth of each

channel is of 1 Herz or less. This approach was proposed in the Project Cyclops report [3] and in a NASA multi-channel spectrum analyzer article [4]. More recent examples of these analyzers have been described in projects Phoenix [5], (1 Hz between 1,000 and 3,000 MHz), SERENDIP IV [6], (168Mchannels, total bandwidth 100MHz), SERENDIP V [7], (128Mchannels, total bandwidth 200MHz).

Many proposals have been made to detect leakage emissions which manifest radio activity of technologically developed civilizations. An estimate of the possibilities of such eavesdropping are given in [8].

It is reasonable to assume that an ETI sends signals not simply to attract attention, but to deliver some useful information, i.e., an ETI sends some modulated signals containing messages. In each epoch we can only use our current technical knowledge to predict what kind of signals an ETI could send. This paper is dedicated to the estimation of the communication transmission rate with ETI in a sphere of radius 1000 light years (ly) which contains $\approx 2.3 \cdot 10^6$ F0 through K7 stars.

The two primary resources for a communication system are transmitter power and channel bandwidth. These two parameters are usually the subject of a tradeoff: one being more precious than the other one. Accordingly, communication systems are classified as being either power-limited or bandwidth-limited. In power-limited systems, coding schemes are used to save power at the expense of bandwidth, whereas in band-limited systems spectrally efficient modulation techniques can be used to save the bandwidth at the expense of the power. In this paper it is assumed that, in the case of SETI, the transmission power is a more precious parameter than the transmission bandwidth, hence the ETI communication system should be classified as *power-limited*.

Un-coded modulation methods are considered: phase-shift keying (PSK) and frequency-shift keying (FSK). Pulse-amplitude modulation (PAM) has inferior characteristics to PSK and FSK and the estimates for PAM are not given here.

Having some plausible estimates of the transmission rate for different modulation schemes we can consider an “inverse” SETI approach: assuming that an ETI uses certain signals (which our civilization would use), for the transmission of information, the pragmatcal solution would be to search for just these kinds of signals using appropriate detection algorithms.

2. The transmission rate

2.1. Radio link power budget

The communication transmission rate is calculated here under the following assumptions:

1. The distance from Earth to an ETI transmitter is $R < 1000ly$.
2. The communication is conducted at S- and X-bands.
3. The transmitter power of ETI is $P_{tr} = 10^{12}W$.
4. The transmitting antenna is omni-directional, i.e., the antenna gain is $G_{tr} = 1$ and effective radiated power (EIRP) is equal to $10^{12}W$.
5. The Arecibo radio telescope has been chosen as the receiver complex: the illuminated diameter of the dish is $d = 225m$, antenna/feed efficiency $\eta = 0.74$, system temperature $T_{sys} = 32$ K which gives the *system equivalent flux density* (SEFD) $\approx 3J$.

2.2. Bit error and transmission rate

The signal-to-noise ratio for the received signal in the bandwidth equal to 1 Hz is

$$SNR_{\text{power}} = \frac{P_{tr}G_{tr}A_{\text{eff}}}{4\pi R^2 k_B T_{\text{sys}}}, \quad k_B = 1.38 \times 10^{-23} \text{ J/K}. \quad (1)$$

The potential transmission bit rate can be estimated using the Shannon's formula for channel information throughput with the bandwidth ΔF and a given SNR as:

$$C = \Delta F \log_2 \left(1 + \frac{SNR_{\text{power}}}{\Delta F} \right). \quad (2)$$

This formula sets a limit on the transmission rate, but not on the error probability. Since the latter is an important characteristic of a communication system, rather than SNR_{power} , another figure of merit is widely used:

$$SNR_{\text{bit}} = SNR_{\text{power}} T_b = \frac{SNR_{\text{power}}}{RW}, \quad (3)$$

where SNR_{bit} is the signal-to-noise ratio per bit, T_b is the duration of signal transmission per 1 bit and RW is the transmission rate. Using this new notation and making the transmission bit rate equal to the channel capacity, $RW = C$, we have:

$$C = \Delta F \log_2 \left(1 + SNR_{\text{bit}} \frac{C}{\Delta F} \right) \quad (4)$$

and

$$SNR_{\text{bit}} = \frac{\Delta F}{C} (2^{C/\Delta F} - 1) \quad (5)$$

If SNR_{bit} becomes small, the ratio $(C/\Delta F) \rightarrow 0$ and the corresponding value $SNR_{\text{bit}} = \frac{1}{\log_2 e} = 0.693$ or, in decibels, $SNR_{\text{bit}} = -1.6$ dB. This value of SNR_{bit} is called the *Shannon limit*.

2.3. PSK

A digital modulation scheme with phase-shift keying (PSK) is widely used in space communication systems [9]. It provides both a low bit-error-rate (BER) and minimum bandwidth. BER for the binary phase-shift keying (BPSK) and for other modulation methods will be calculated using the formulas in Appendix A.

Quadri-phase shift keying (M-ary phase modulation, $M = 4$), denoted as QPSK, has the same bit-error performance as BPSK, but the equivalent bit rate is two times higher than that of BPSK.

To obtain $BER = 10^{-5}$ for un-coded BPSK the necessary $SNR_{\text{bit}, BER=10^{-5}}$ must be equal to 9.6 dB (or 9.0945). Therefore, the ratio $SNR_{\text{power}}/SNR_{\text{bit}, BER=10^{-5}}$ gives the transmission rate achievable for a given SNR_{power} as a function of $P_{tr}, G_{tr}, R, A_{eff}$ for the value $BER = 10^{-5}$.

Fig. 1 demonstrates how the transmission rate depends upon the distance (in light years) for the Arecibo radio telescope and $BER = 10^{-5}$, $P_{tr} = 10^{12}$ W, $G_{tr} = 1$. The upper curve corresponds to the Shannon limit. The three closely running curves below correspond to PSK, coherent and non-coherent differential PSK (DPSK), respectively. For the coherent DPSK $SNR_{\text{bit}, BER=10^{-5}} = 9.76$ and for the non-coherent DPSK $SNR_{\text{bit}, BER=10^{-5}} = 10.82$, [11]. There is no significant difference between these three curves, i.e., DPSK is only slightly inferior to PSK. DPSK does not require an elaborate method for estimating the carrier phase and it is often used in digital communication systems.

Table 1 contains the values of transmission rate corresponding to these three curves.

The lower collection of curves (PSK and two DPSK) corresponds to the more realistic situation when scattering and multi-path caused by the interstellar medium is taken into account, [12]. This effect broadens the sinusoidal signal up to the bandwidth $df_{\text{min}} = 0.01$ to $0.05 Hz$. Therefore, the assumption for the average interval $T_{\text{average}}, 1/T_{\text{average}} = \Delta f_{\text{average}} \approx 1/T_{\text{bit}}$ is not valid after $\Delta f_{\text{average}} < df_{\text{min}}$. Limiting the bandwidth by the value

Table 1: The transmission rate bit/sec as a function of distance for un-coded PSK, transmitter $EIRP = 10^{12}W$ and Arecibo-like receiver antenna, $SEFD = 3J$, $BER = 10^{-5}$.

	Distance, light years				
PSK	10	50	100	500	1000
coherent BPSK,	64.7	2.56	0.65	0.026	$6.5 \cdot 10^{-3}$
coherent DPSK	60.3	2.4	0.60	0.024	$6.0 \cdot 10^{-3}$
non-coherent DPSK	54.4	2.17	0.544	0.022	$5.4 \cdot 10^{-3}$

df_{min} worsens the $SNR_{bit} = SNR_{power}T_b/\sqrt{df_{min}T_b} = SNR_{power}\sqrt{T_b/df_{min}}$. Therefore, the transmission rate for $df_{min} > 1/T_b = RW$ must be calculated as follows:

$$RW = \left(\frac{SNR_{power}}{SNR_{bit, BER=10^{-5}}}\right)^2 \frac{1}{df_{min}} \quad (6)$$

The breakdown visible in Fig. 1 corresponds to $df_{min} = 0.05Hz$, i.e., in the case of very long ($> 20s$) narrow-band signals used for communication the transmission rate is significantly lower than the potential one.

Fig. 1 depicts the situation with the omni-directional transmitting antenna. When both transmitter and receiver sides know each other's coordinates (targeted communication), a directional transmitting antenna similar to the receiver antenna (Arecibo in our example) can significantly increase the communication distance, see Fig. 2. The large antenna gain G_{tr} at 1GHz allows for communication to several Mly.

A considerable gain in BER performance can be achieved using special coding of the bit stream before modulation. For example, for binary modulation and $P_B = 10^{-5}$ the error performance of turbo code is within 1.8 dB of the Shannon limit. But it is difficult to guess the coding scheme used by ETI, therefore, the performance of communication is calculated here for un-coded signals only.

The first phase of SKA presumes $SEFD = 2.7J$ (250 dishes, each 15m diameter, antenna-feed efficiency $\eta = 0.7$, $T_{sys} = 30K$), [13]. This is comparable with Arecibo, but the field-of-view is $1.37deg^2$ at 1GHz which in combination with multi-beaming allows for a faster all-sky survey. The full SKA is to consist of 1500 dishes [14], but the core (25%) will have $SEFD = 1.785J$ which will increase the transmission rate by 1.68 times.

2.4. FSK

As was mentioned at the end of the Introduction the transmission power is a more precious parameter than is the transmission bandwidth in ETI communication. Using of $M = 2^k$ orthogonal signals can increase the necessary bandwidth but it requires smaller SNR_{bit} to achieve a given error probability with FSK. M-ary PSK provides better bits-per-second-per-hertz-of-bandwidth ratio but $SNR_{bit, BER=10^{-5}}$ for $M=8, 16$ and 32 is $19.8, 55.4$ and 171.2 , respectively. The same tendency exists for M-ary PAM (pulse amplitude modulation) and M-ary QAM (quadrature amplitude modulation).

The situation is different for frequency shift keying (FSK) signals. Each symbol corresponding to a particular binary sequence of the length k is transmitted on one of the m -th frequencies during an interval T :

$$s_m(t) = A \cos[2\pi(f_c + m\Delta f)t], 0 \leq t \leq T, m = 1, 2, \dots, M, \quad (7)$$

where $\Delta f = 1/2T$, T – is the duration of a symbol. For example, for $k = 5$, there are 32 different orthogonal signals, each at its own frequency. The total bandwidth is $W = M\Delta f$. The effective transmission rate is $RW = k/T$, $k = \log_2 M$. The ratio RW/W is called *bandwidth expansion*: $RW/W = (2\log_2 M)/M$. Theoretically, by increasing M it is possible to reach the Shannon limit.

Un-coded M-ary frequency shift keying (MFSK) gives a higher transmission rate than an un-coded BPSK for a fixed $BER=10^{-5}$ and $M \geq 8$. MFSK requires a wider bandwidth than BPSK but this resource is of less importance than transmitter power.

Fig. 3 shows the transmission rate as a function of distance for un-coded *coherent* MFSK, transmitter $EIRP = 10^{12}W$ and Arecibo-like receiver antenna, $SEFD = 3J$, $BER = 10^{-5}$. Bandwidth constraint due to interstellar propagation is $\Delta f_{min} = 0.05Hz$. The Shannon limit is the upper curve. The lower curve corresponds to $M=2$ and the following curves correspond to $M=4, 8, 16, 32$ and 64 , respectively. The breakdown due to the loss of effectiveness in averaging is clearly visible.

All formulas used for calculation (see Appendix A) contain SNR_{bit} or SNR_{symbol} which, in their turn, depend on the *energy* spent during the transmission. Having a constant transmitter power P_{tr} , the larger the distance, the longer the necessary duration of the elementary signal. Another option is to keep the energy per symbol constant. With this approach the duration T of the signal can be shorter than $1/\Delta f_{min}$ whereas the P_{tr} is larger. This

transition to the shorter, pulse-like signals with a duration of less than 20 to 100s means that the breakdown due to Δf_{min} can be avoided.

Fig. 4 shows the transmission rate as a function of distance for un-coded *non-coherent* MFSK, the same Arecibo-like receiver antenna, $SEFD = 3J$, $BER = 10^{-5}$. The Shannon limit is represented by the upper curve, the lower curve corresponds to $M=2$ and the subsequent curves correspond to $M=4,8,16,32$ and 64 , respectively. The transmission rate for non-coherent MFSK is slightly less than for the coherent MFSK, Fig. 3.

There is no breakdown due to Δf_{min} in Fig. 4 deliberately in order to show the run of the curves in the absence of this effect and assuming that the transmitter keeps the transmission energy per symbol constant, i.e., the duration of the symbol is limited by $1/\Delta f_{min}$.

Table 2 contains the values of transmission rate corresponding to Fig. 4.

Table 2: The transmission rate in bit/sec as a function of distance for un-coded non-coherent MFSK, transmitter $EIRP = 10^{12}W$ and Arecibo-like receiver antenna, $SEFD = 3J$, $BER = 10^{-5}$.

Distance, light years					
MFSK	10	50	100	500	1000
M=2	27.2	1.09	0.27	0.01	$2.7 \cdot 10^{-3}$
M=4	51.2	2.05	0.51	0.02	$5.1 \cdot 10^{-3}$
M=8	72.5	2.9	0.725	0.03	$7.0 \cdot 10^{-3}$
M=16	91.6	3.66	0.92	0.037	$9.0 \cdot 10^{-3}$
M=32	108.8	4.35	1.09	0.044	0.011
M=64	124	5.0	1.24	0.05	0.012

3. Pattern detection

The estimates of transmission rate given in the previous section support the presumption that it is energetically advantageous to use MFSK, i.e., detection attempts can be focused on the search for narrow-band pulses scattered at different frequencies. The duration of the pulses can be of the order of 20 to 100s ($\Delta f_{min} = 0.05$ to $0.01Hz$) or longer (if reconciled with the necessity of long intervals of averaging,[15]). These signals are detectable on the time-frequency plane as random, non-intersecting parallel tracks. The slope of the tracks depends upon the Doppler frequency drift which might not be compensated for at either transmitter or receiver side. An artificial additional slope can even be deliberately introduced by ETI to emphasize its artificial origin. Computer simulation was made to provide an example of such a pattern which is shown in the upper panel of Fig. 5.

One of the possible methods of detection of such a pattern is to apply the Hough transform (HT) which is widely used in image processing for line detection [16]. Details of HT and examples of computer simulation are given in Appendix B. Here the detection of straight line tracks in the time-frequency plane with the help of HT is demonstrated.

The lower panel of Fig. 5 shows the result of HT as applied to the binary version (after thresholding) of the image in the upper panel. The three peaks correspond to the three lines in the upper panel. The angle coordinate θ corresponding to the frequency drift (slope) is the same for all three peaks. The ρ -coordinates depict the difference in carrier frequencies. No *a priori* information was used for detection: neither for the positions or durations of pulses or the slope of the lines.

When the track of a pulse in the time-frequency plane cannot be approximated by a straight line, HT can be modified to detect a second order curve. There are many versions of HT adapted to the detection of particular curves. The example in Appendix B (Fig. B.8) demonstrates the usage of HT for de-dispersion in the case of interstellar dispersion.

An additional useful property of the HT is the accumulating of a number of points belonging to the same line, which is, in essence, averaging. Having the track of a pulse somewhere on the time-frequency plane it is possible also to detect a weak pulse using this averaging property of HT, [17].

4. Conclusions

1. Frequency-shift keying can be a method of modulation used by ETI. For long distances the low bit rate ($< 0.01 \text{ bit/sec}$) requires a long time on target to accumulate the necessary energy for the receiver. Modern SETI spectrum analyzers are well suited to searching for these types of signals.

2. Scattering and multi-path caused by the interstellar medium broadens the sinusoidal signal up to the bandwidth $df_{min} = 0.01$ to 0.05 Hz . This means that averaging of CW for time intervals $> 1/df_{min}$ sec must be performed in the bandwidth $\approx df_{min}$ which makes the transmission rate substantially slower. Pulse signals with the same energy but shorter than $1/df_{min}$ (20 to 100 seconds) avoid this obstacle, because transmission of information by narrow-band pulses with the same average energy budget provides the same transmission bit rate. This can therefore be one of the reasons to search for the narrow-band pulse-like signals from ETI.

3. Transmission power of 10^{12} W , which is equal to 10^{-5} of the Solar radiation power coming to the Earth's surface, is enough to receive digital information with antennas such as Arecibo and SKA with a transmission rate $RW \approx 10^{-2} \text{ bit/s}$ at a distance of 1000ly and an omni-directional transmitting antenna. A transmission rate equal to 10^{-2} bit/s allows transmission of the full code of human genome ($1.2 \cdot 10^{10} \text{ bits}$) from a distance of 1000ly in $1.2 \cdot 10^{12} \text{ s} = 1.2 \cdot 10^5 \text{ years}$, significantly less than the time taken by natural evolution on Earth: $\approx 10^9 \text{ years}$.

If an ETI were able to dispose of n times larger transmission power, the transmission rate will proportionally increase.

4. The Hough transform can be a useful tool for detecting patterns in the time-frequency plane where there is uncertainty about the duration and frequency drift of narrow-band pulses.

Appendix A. Formulas for the bit-error-rate

1. The probability of bit error for binary phase-shift keying (BPSK), [11], BER can be estimated as follows:

$$P_{\text{BER,BPSK}} = Q(\sqrt{2 \times SNR_{\text{bit}}}), \quad (\text{A.1})$$

where

$$Q(x) = \frac{1}{\sqrt{2\pi}} \int_x^\infty e^{-\frac{t^2}{2}} dt, \quad (\text{A.2})$$

$SNR_{\text{bit}} = SNR_{\text{power}} \times T_{\text{bit}} = \frac{SNR_{\text{power}}}{RW}$ is the signal-to-noise ratio per bit, T_{bit} is the duration of signal transmission per 1 bit and $RW = 1/T_{\text{bit}}$ is the transmission rate.

2. The probability of bit error for coherent differential PSK (DPSK) is

$$P_{BER,DPSK} = 2Q(\sqrt{2 \times SNR_{\text{bit}}})[1 - Q(\sqrt{2 \times SNR_{\text{bit}}})] \quad (\text{A.3})$$

3. The probability of bit error for non-coherent differential PSK is

$$P_{BER,noncorDPSK} = 0.5 \exp(-SNR_{\text{bit}}) \quad (\text{A.4})$$

4. The probability of bit error for M-ary PSK

$$P_{BER,MPSK} = \frac{1}{k} 2Q(\sqrt{2kSNR_{\text{bit}} \sin \frac{\pi}{M}}) \quad (\text{A.5})$$

5. The probability of bit error for the *coherent* processing of $M = 2^k$ orthogonal signals (MFSK) can be calculated using the following expression ([10], p. 259):

$$P_{\text{BER,FSK}_C} = \frac{2^{k-1}}{2^k - 1} \cdot \frac{1}{\sqrt{2\pi}} \int_{-\infty}^{\infty} [1 - (\frac{1}{\sqrt{2\pi}} \int_{-\infty}^y e^{-\frac{t^2}{2}} dt)^{M-1}] \times \\ \times \exp[-(y - \sqrt{2 \cdot SNR_{\text{symbol,FSK}}})^2/2] dy, \quad (\text{A.6})$$

where $SNR_{\text{symbol,FSK}} = SNR_{\text{power}} \times T$, each signal transmits k bits simultaneously.

6. The probability of bit error for the *noncoherent* processing of $M = 2^k$ orthogonal signals is calculated using the following expression ([10], p. 310):

$$P_{\text{BER,FSK}_{NC}} = \frac{2^{k-1}}{2^k - 1} \sum_{n=1}^{M-1} (-1)^{n+1} \binom{M-1}{n} \times \\ \frac{1}{n+1} \exp[-nkSNR_{\text{symbol,FSK}}/(n+1)]. \quad (\text{A.7})$$

Appendix B. The Hough Transform

The Hough Transform (HT) is a useful algorithm for the detection of straight lines in binary images when the amplitudes of pixels are equal to

two numbers, for example, 1 or 0. Each straight line $y = ax + b$ in a plane can be parameterized by the angle θ of its normal to the horizontal axis and its distance ρ from the origin of coordinates. The equation of a line is

$$y = -x \frac{\cos(\theta)}{\sin(\theta)} + \frac{\rho}{\sin(\theta)}. \quad (\text{B.1})$$

This equation can be rewritten for ρ as a function of (x, y) :

$$\rho = x \cos(\theta) + y \sin(\theta). \quad (\text{B.2})$$

A line can then be transformed into a single point in the parameter space (ρ, θ) which is called the Hough space. For any pixel in the image with position (x, y) , an infinite number of lines can go through that single pixel. By using equation (B.2) all pixels belonging to the line can be transformed into the Hough space. A pixel is transformed into a sinusoidal curve that is unique for this pixel. Doing the same transformation for another pixel gives another curve that intersects the first curve at one point in the Hough space. This point represents the straight line in the image space that goes through both pixels. This operation is repeated for all pixels of the image. The pixels belonging to the same straight line have the same point of intersection in the Hough space.

For each point in the Hough space the HT program assigns a counter which accumulates the number of these intersections. Therefore, if there is a straight line with the parameters (ρ_i, θ_j) consisting of n pixels the counter corresponding to the point (i, j) in the Hough space will contain number n . This is correct only for the ideal case when there is no noise in the image. In the case of a noisy image the situation is as follows.

Let the time-frequency plane be the image on which the search for signal patterns is performed. Each line of pixels along the time axis represents “intensity” samples at the i -th output of the spectrum analyzer’s filter bank. In the absence of a signal pattern, these samples are random numbers - often with a Gaussian pdf due to preliminary averaging. A binary image is created using the threshold thr equal to $thr \approx \sigma + m$ where σ is the *rms* of the noise samples and m is the mean value. If the amplitude of a sample is less than thr it is converted to 0, otherwise it is equal to 1. The binary image is covered with the random 0 and 1.

To better understand the HT a computer simulation example is given here. Let the 400×400 image in Fig. B.6, upper panel, represent the “noisy”

time-frequency plane. Each horizontal line consists of $N = 400$ samples of the total power outputs of the filter bank assigned to the frequencies from 0 to 160Hz. Each sample corresponds to the integration time $2000/N = 5s$. The narrow-band signal is the input of the filter bank: with a frequency drift and the noise - $x(t) = S\cos[2\pi(F_0 + kf \cdot t)t] + n(t)$, the noise $n(t)$ is represented by random numbers with the normal distribution $\mathcal{N}(0,1)$, $S = 0.2$. The lower panel of Fig. B.6 shows the HT of the binary 400×400 image obtained from the image in the upper panel after thresholding equal to 0.9 of the noise *rms*. The origin of coordinates is in the centre of the image. The peak due to the signal track has coordinates $\rho = -6$ (in pixels) and $\theta = -9.45^\circ$ which correspond to the $F_0 = 64.4Hz$ and $kf = 0.0135Hz/s$.

Another example in Fig. B.7, upper panel, illustrates a wide-band pulse signal in the time-frequency plane with a different frequency drift and the outputs of the same filter bank are simulated. The HT is shown in the lower panel of Fig. B.7. The peak corresponds to $F_0 = 81Hz$ and frequency drift slope $kf_t = -0.02Hz/s$.

The last example of the Hough transform application is given in Fig. B.8 when the signal track on the time-frequency plane is not linear: the interstellar dispersion is calculated with the formula:

$$t_{delay}(f) = t_0(f_1) + 4.15DM[\frac{1}{f^2} - \frac{1}{f_1^2}], \quad (B.3)$$

where t_{delay} — in msec, f_1 , f in GHz, and DM in pc/cm^3 . Fig. B.8, upper panel, demonstrates a computer simulation of the pulse's spectrum with this kind of dispersion in the frequency range 0.05 to 0.1GHz. The parameter space for HT in this case is $[DM, t_0(f_1)]$, i.e., the dispersion measure and the delay at the frequency $f_1 = 0.1GHz$. The coordinates of the peak in the HT plane in Fig. B.8, lower panel, correspond to $DM = 18.04pc/cm^3$ and $dt_0 = 2400ms$.

References

- [1] J. C. Tarter, The Search for Extraterrestrial Intelligence (SETI), Annu. Rev. Astron. Astrophys., 39 (2001), 511548.
- [2] R. D. Ekers, D. K. Cullers (Eds.) SETI 2020: A Roadmap for SETI, SETI Press, 2002.

- [3] NASA. Project Cyclops, Publ. CR114445, NASA, Moffett Field, Calif., 1973.
- [4] D. K. Cullers, I. R. Linscott and B. M. Oliver, Signal Processing in SETI, Communications of ACM, 1985, 28, 1151-1163.
- [5] J. W. Dreher, The Phoenix Signal Detection System, Acta Astronautica, 1998, 42, 635-640.
- [6] [http : //seti.berkeley.edu/sites/default/files/SERENDIP_IV_DataAcquisition_Reduction_and_Analysis_ASP213_2000.pdf](http://seti.berkeley.edu/sites/default/files/SERENDIP_IV_DataAcquisition_Reduction_and_Analysis_ASP213_2000.pdf)
- [7] [http : //casper.berkeley.edu/wiki/SETI_Spectrometer](http://casper.berkeley.edu/wiki/SETI_Spectrometer)
- [8] J. C. Tarter, Astrobiology and SETI, New Astron. Rev., 2004, 48, 1543-1549.
- [9] J. H. Yuen et al. Modulation and Coding for Satellite and Space Communications, Proc. IEEE, 1990, 78, 1250
- [10] J. G. Proakis, Digital Communications, Fourth Ed., 2001, McGraw Hill Higher Education, ch. 5.
- [11] Y. Okunev, Phase and Phase-Difference Modulation in Digital Communications, 1997, Artech House, ch. 6.
- [12] J. M. Cordes and T. J. Lazio, Interstellar Scattering Effects on the Detection of Narrow-Band Signals, Astrophys. J., 1991, 376 , 123
- [13] P. Dewdney et. al. SKA Phase 1: Preliminary System Description, SKA Memo 130, Nov. 2010.
- [14] A. J. Faulkner, SKADS White Paper in S.A. Torchinsky et al. (Eds.) Widefield Science and Technology for the SKA, SKADS Conference 2009, 24-29.
- [15] N. T. Petrovich, Astrophys. and Space Sci., 1997, 252, 55-66.
- [16] R. O. Duda and P. E. Hart, 1973, Pattern Classification and Scene Analysis, Wiley, New York
- [17] P. A. Fridman, A method of Detection of Radio Transients, Mon. Not. Roy. Astr. Soc., 2010, 409, 808-820.

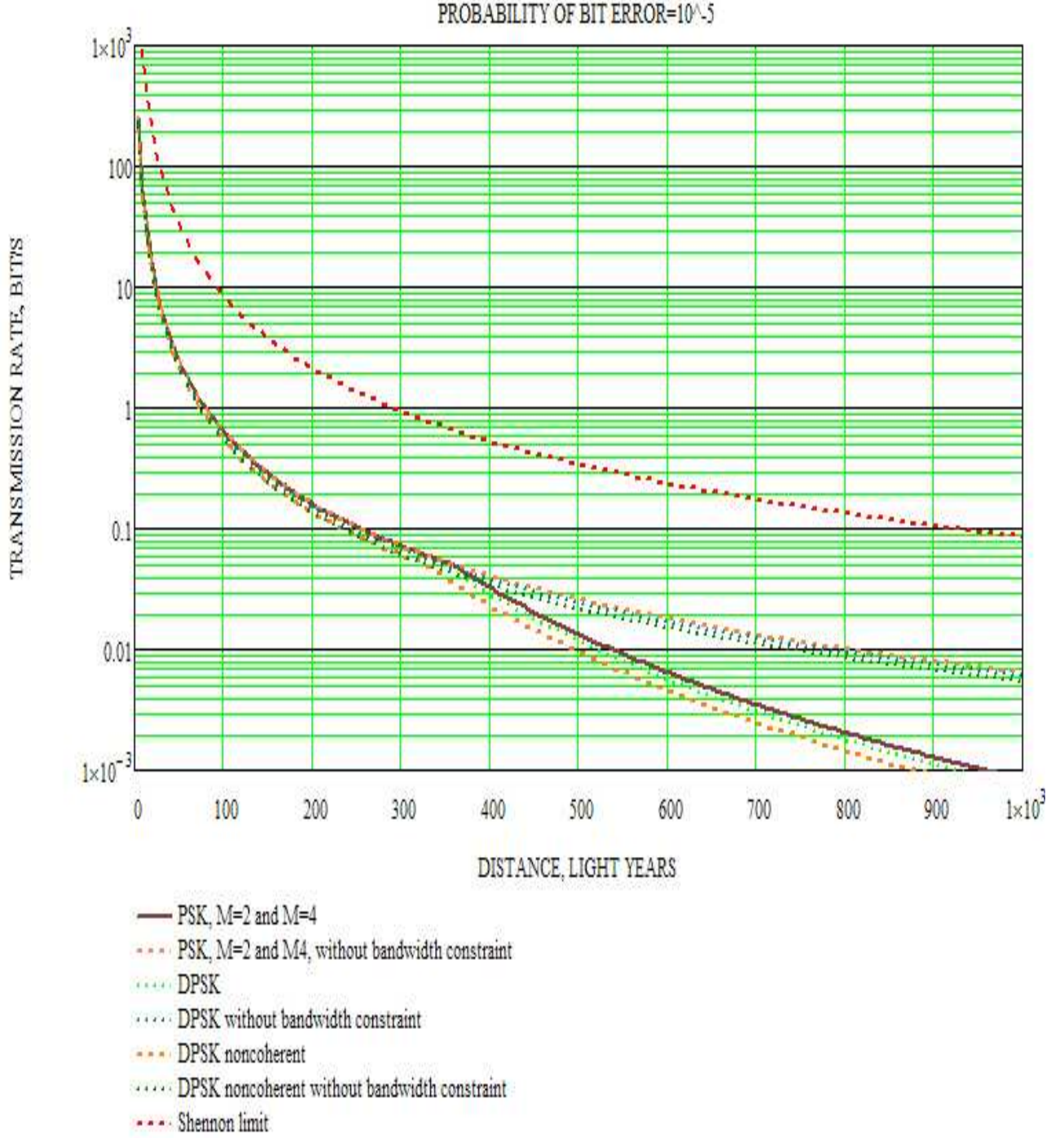


Figure 1: The transmission rate as a function of distance for un-coded PSK, transmitter $EIRP = 10^{12}W$ (transmitting power= $10^{12}W$ and omnidirectional antenna) and Arecibo-like receiver antenna, $SEFD = 3J$, $BER = 10^{-5}$. The top curve shows the Shannon limit (best possible rate). Breakdowns in two collections of curves (PSK, DPSK and noncoherent DPSK) are produced by bandwidth constraint due to interstellar propagation at $\Delta f_{min} = 0.05Hz$.

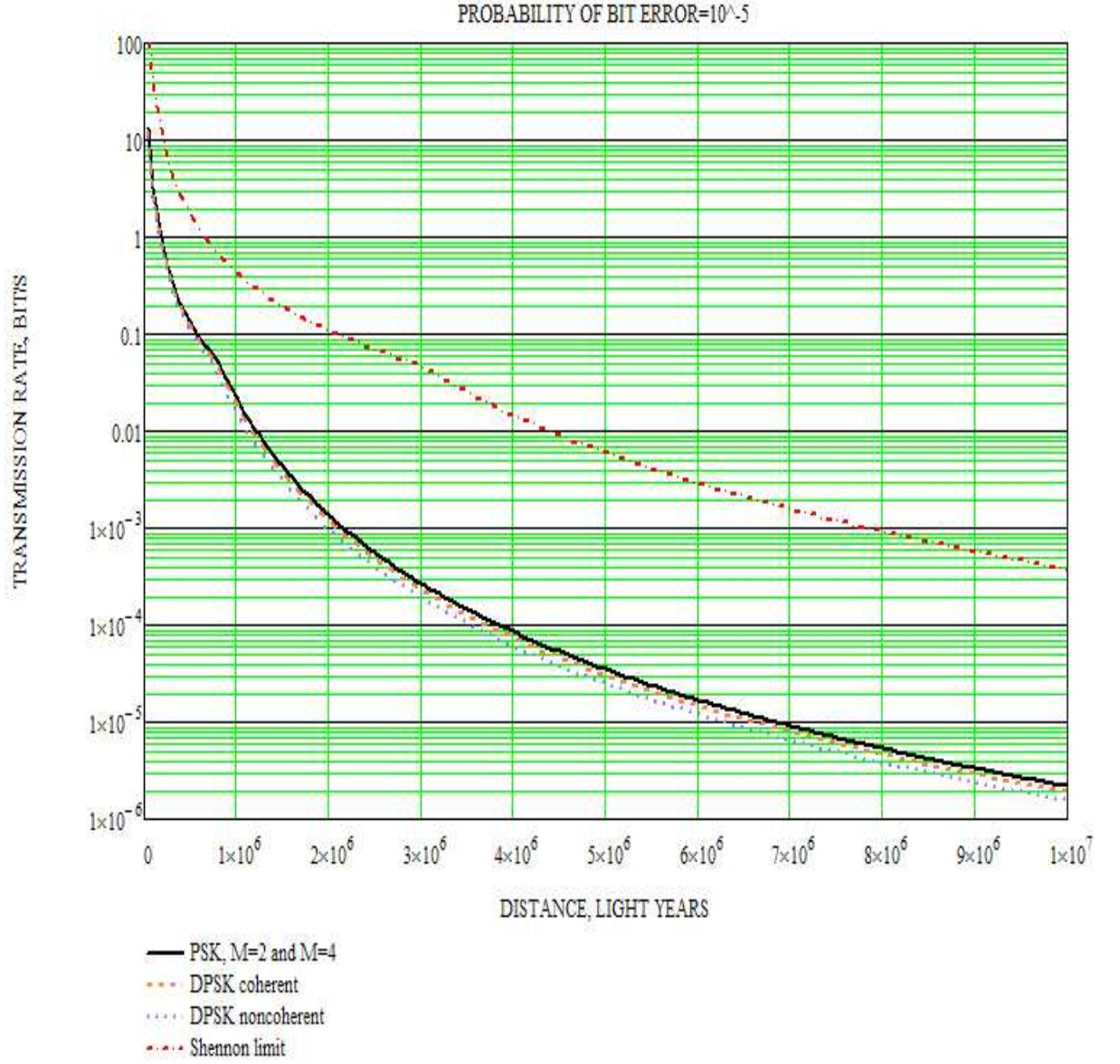


Figure 2: The increase in transmission rate using a high gain Arecibo-like transmitting antenna. Other parameters as in Fig. 1. Note the change in scale on both axes. The bandwidth constraint due to the interstellar propagation is $\Delta f_{min} = 0.05 Hz$.

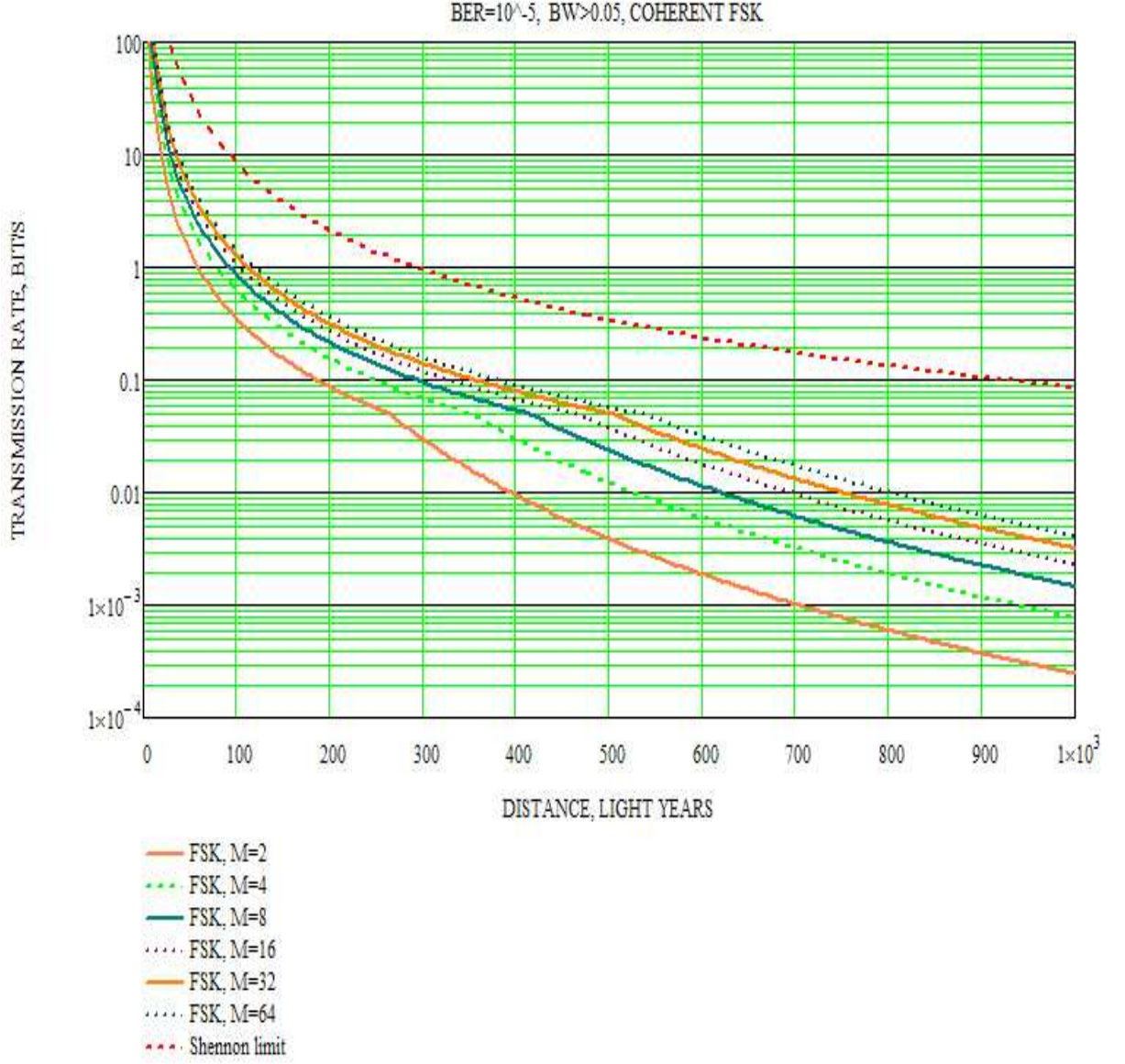


Figure 3: The transmission rate as a function of distance for un-coded coherent MFSK, transmitter $EIRP = 10^{12}W$ and Arecibo-like receiver antenna, $SEFD = 3J$, $BER = 10^{-5}$. The bandwidth constraint due to the interstellar propagation is $\Delta f_{min} = 0.05Hz$; note the resulting break at 0.05 bits/s.

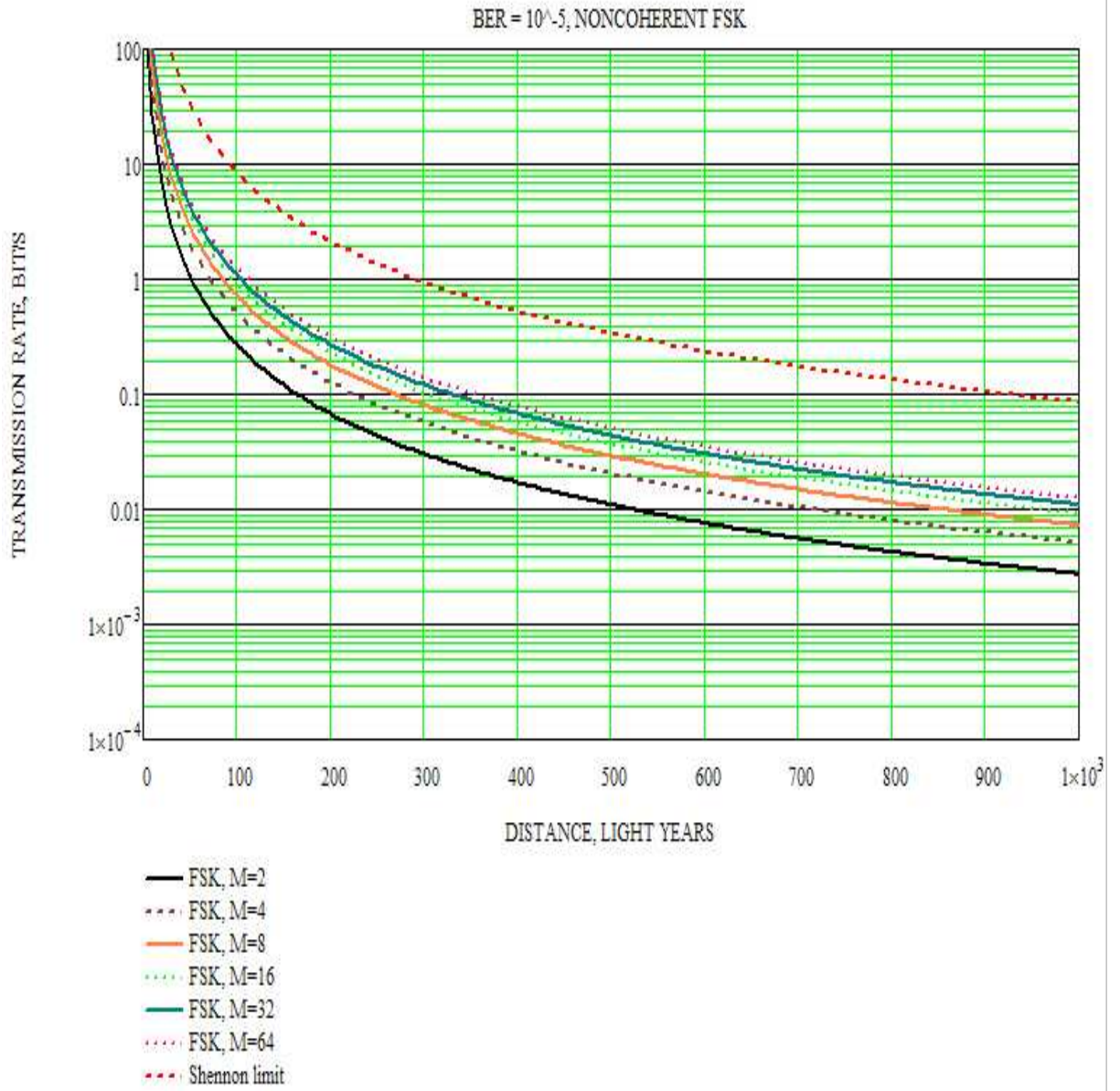


Figure 4: The transmission rate as a function of distance for un-coded non-coherent MFSK, transmitter $EIRP = 10^{12}W$ and Arecibo-like receiver antenna, $SEFD = 3J$, $BER = 10^{-5}$. Interstellar broadening effects are avoided by limiting pulse durations to less than 20 s, leading to higher transmission rates.

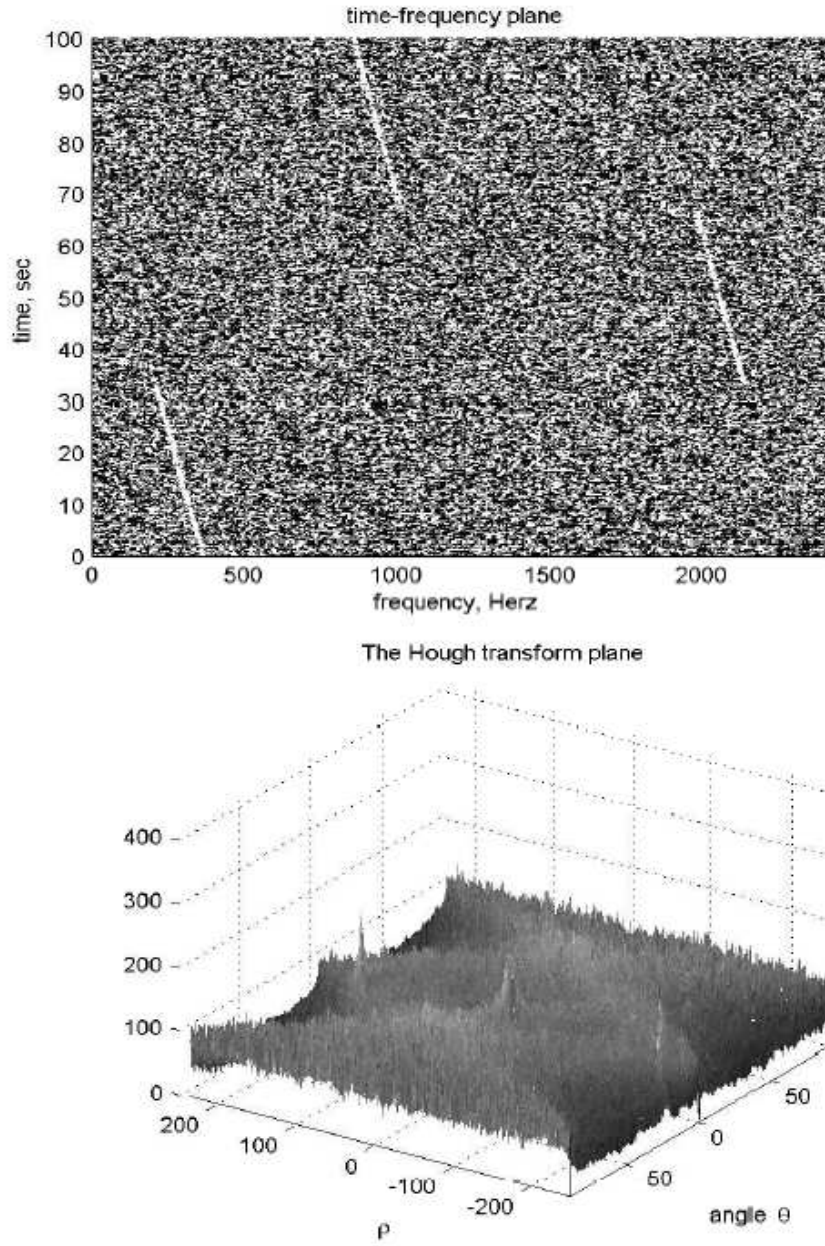


Figure 5: Upper panel: three narrow-band impulses in the time-frequency plane imitate FSK signals. The lower panel: after the Hough transform, three peaks correspond to the three lines in the upper panel. The angle coordinate θ corresponding to the frequency drift is the same for all three peaks. The ρ -coordinates depict the difference in the carrier frequencies.

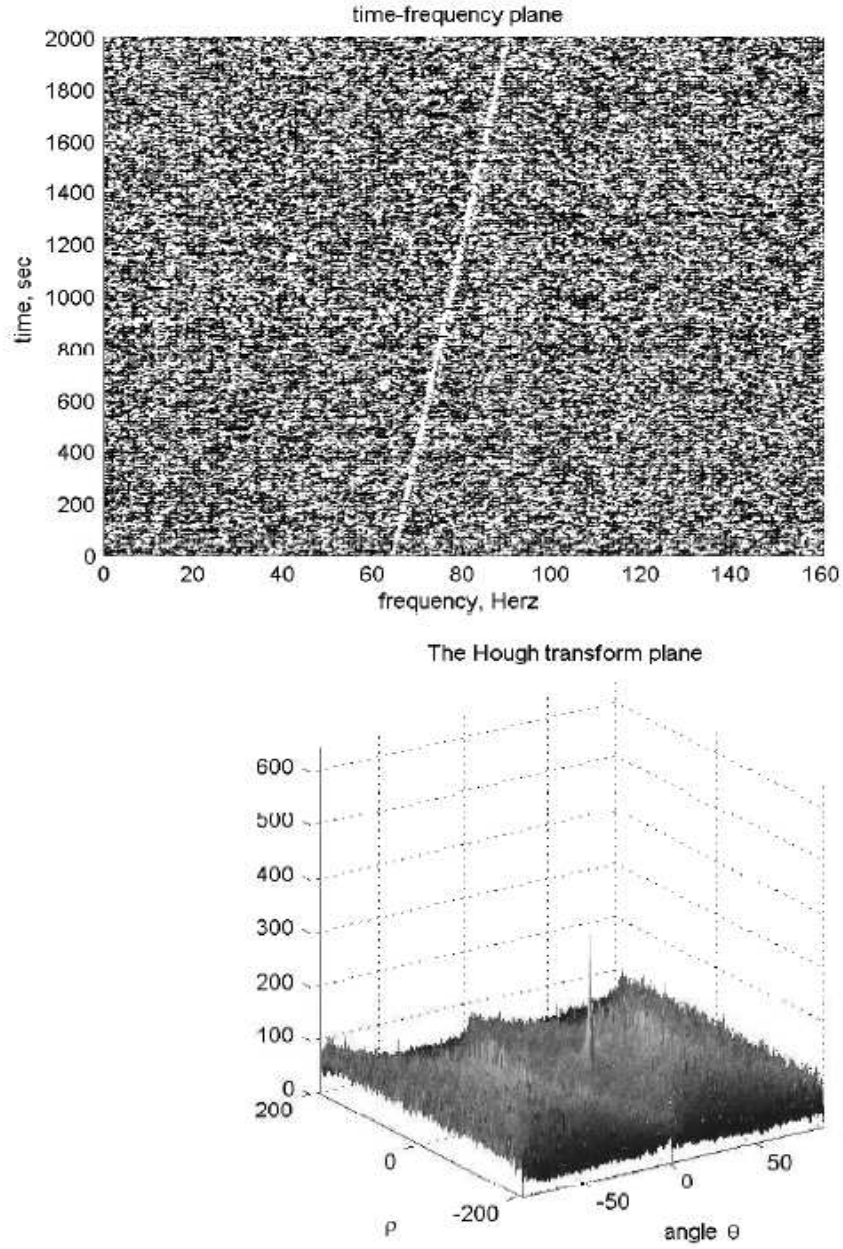


Figure B.6: The upper panel - time-frequency plane with the drifted narrow-band signal plus Gaussian noise, the lower panel-the Hough transform. The peak corresponds to $F_0 = 64.4Hz$ and frequency drift slope $k f_t = 0.0135Hz/s$.

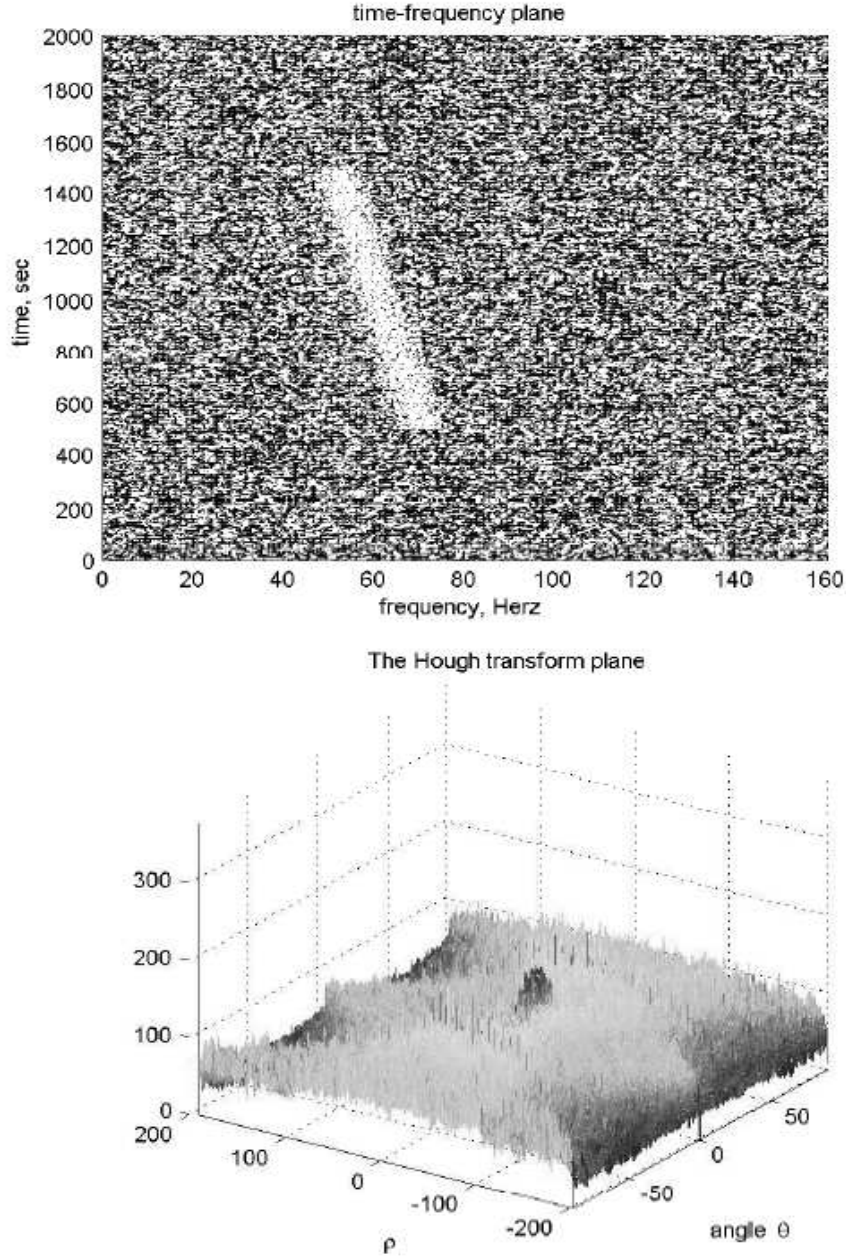


Figure B.7: The upper panel similar to Fig. B.6 signal track in the time-frequency plane but with the wider spectrum and different frequency drift; the lower panel - the Hough transform. The peak corresponds to $F_0 = 81Hz$ and frequency drift slope $k f_t = -0.02Hz/s$.

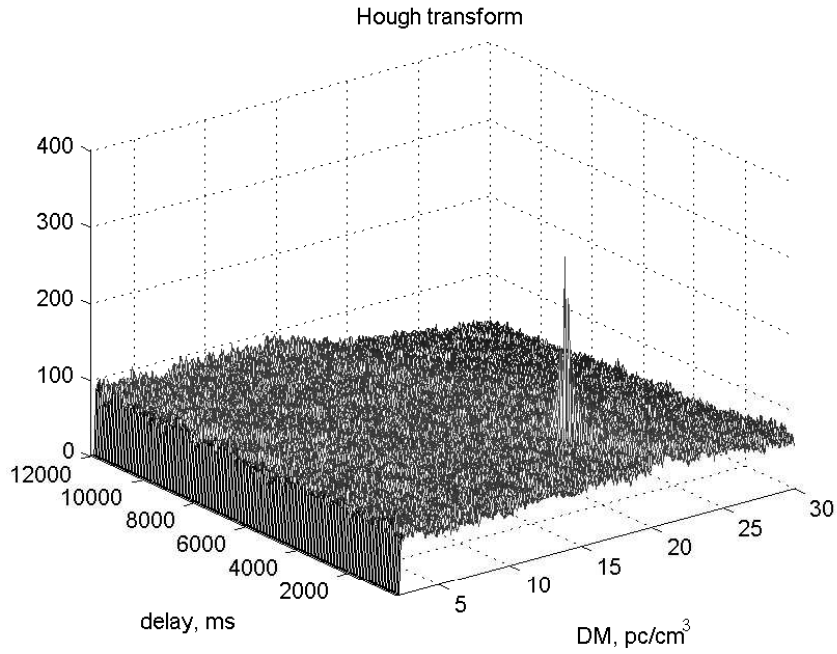
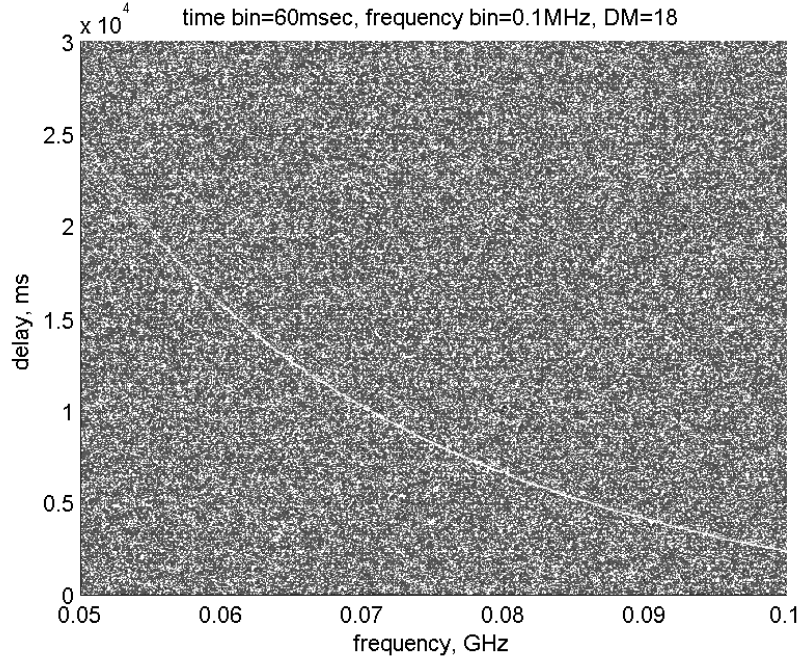


Figure B.8: The upper panel - pulse track with dispersion (formula (B.2)) in the time-frequency plane. Two parameters: dispersion measure DM and delay at frequency 0.05GHz dt_0 determine the position of the curve. The lower panel - the Hough transform. The coordinates of the peak correspond to $DM = 18.04\text{pc/cm}^3$ and $dt_0 = 2400\text{ms}$.